An Acad Bras Cienc (2022) 94(Suppl. 1): e20210600 DOI 10.1590/0001-3765202220210600
Anais da Academia Brasileira de Ciências | *Annals of the Brazilian Academy of Sciences*
Printed ISSN 0001-3765 I Online ISSN 1678-2690
www.scielo.br/aabc | www.fb.com/aabcjournal

GEOSCIENCES

Highlights of ionospheric investigations at Comandante Ferraz Brazilian Antarctic Station

EMILIA CORREIA, JOSÉ HENRIQUE FERNANDEZ, JOSÉ VALENTIN BAGESTON, EDUARDO P. MACHO & LUÍS TIAGO M. RAUNHEITTE

Abstract: The ionospheric investigations have improved our understanding of the space weather role in the upper atmosphere conditions, particularly at higher latitudes where the geospace phenomena print their signatures. The simultaneous observations using multi-instruments have improved our knowledge of the coupling processes inside the ionosphere, and their connection with the magnetosphere and neutral atmosphere processes under the space weather phenomena. The ionosphere probing at EACF started on 1986 using an analogical very low frequency (VLF) system, and after the year 2004 using digital VLF system, global navigation satellite system (GNSS), riometers and Canadian digital ionosonde (CADI). This paper presents the different radio techniques that have been used at Brazilian Antarctic Station Comandante Ferraz (EACF) to characterize the ionospheric conditions, and the highlights of the studies using multi-instrument observations performed in the last few decades.

Key words: ionosphere, Antarctica, Sun-Earth interactions, atmospheric waves, atmosphere coupling, geospace connections.

INTRODUCTION

The Earth´s atmosphere is mainly controlled and modified by the Sun energy, and particularly the upper ionized atmosphere, the ionosphere, is formed due to the strong molecular absorption of the ultraviolet radiation range at heights from 60 to 1000 km. The solar ionizing radiation shows a 11-year strong ultraviolet variation, associated with the number of sunspots, which changes the ionospheric physical-chemical properties. At higher latitudes, the ionosphere is also impacted by the energetic particles of the solar wind and cosmic ray's incomings from the outer space. So, the ionosphere is disturbed by solar-driven processes, as the strong enhancement of the radiation during the solar flares and by the impact of geoeffective coronal mass ejections (CMEs), which causes the geomagnetic storms. But even during quiet geomagnetic periods the ionosphere is disturbed by electrodynamic processes, driven by plasma drifts produced by the thermospheric neutral winds (e.g., Heelis 2004). The effect of the dynamics of neutral atmosphere is most pronounced during the winter season, when the ionosphere electron density shows fluctuations produced by the upward propagation of gravity and planetary waves originated at the troposphere (Lastovicka 2006).

The investigation of the ionospheric external drives at high latitudes has received special attention because there, the ionosphere has a direct connection with the outer space phenomena. Since the ionospheric disturbances cover large spatial scales, extending from high to lower latitudes, the investigations at EACF have been using instrumentation networks

operating in Antarctica and South America, involving national and international scientific collaborations.

Nowadays, the characterization of the ionospheric disturbances is of great relevance because they affect the propagation of radio signals used in high frequency (HF) communication and global navigation satellite systems (GNSS), widely used in the modern society; as well as in more critical situations like in satellite control, air and ground traffic control, petrol platforms stabilization and precision agriculture. Here, we present the instrumentation and the main scientific results of the ionospheric investigations developed at Comandante Ferraz Brazilian Antarctic Station (EACF - 62.1°S, 58.4°W) during the last few decades.

MATERIALS AND METHODS

The characterization of the ionospheric conditions has been done at EACF using simultaneously a variety of radio sounding techniques, which permits to determine the ionospheric conditions at different heights, from 70 to ~400 km. In the following we describe the main radio techniques and the methodologies used at EACF.

Very low frequency (VLF)

The VLF measurements at EACF started in 1986 using an analog TRACOR receiver to detect the amplitude and phase of the signals; after 1995, VLF amplitude measurements with 20ms time resolution were performed using a Stanford MSK receiver (Johnson et al. 1999). From 2006, the VLF amplitude and phase measurements with 10ms time resolution have been done digitally using an Atmospheric Weather Electromagnetic System for Observation, Modeling and Education receiver - AWESOME (Scherrer et al. 2008, Cohen et al. 2010), which also records broad-band data in the VLF frequency range. The VLF measurements at EACF are complemented with another AWESOME receiver operating at Radio Observatory of Itapetinga (ROI, 23.2°S, 46.5°W) in São Paulo, and by the South America VLF Network (SAVNET, Raulin et al. 2009) that detects VLF amplitude and phase with 1s time resolution.

The main VLF transmitter stations tracked are: the US Navy, namely the Maine (NAA, 24 kHz, 44.6°N - 67.3°W); Washington (NLK, 24.8kHz, 48.2°N - 121.9°W); Hawaii (NPM, 21.4kHz, 20.4°N, 158.2°W); North Dakota (NLM, 25.2kHz, 46.3°N - 98.3°W) and Puerto Rico (NAU, 40.75kHz, 18.4°N - 67.1°W), and North West Cape in Australia (NWC, 19.8 kHz, 21.8°S - 114.2°E). The large spatial distribution of VLF paths between the transmitter and receiver stations permits to investigate the ionosphere from low to higher latitudes, including the magnetic equator and South Atlantic Magnetic Anomaly (SAMA) regions.

VLF radio sounding technique is used to investigate the low ionosphere, that is, D- and E-regions, where the radio signals ranging from 1 to 50 kHz are reflected in such regions and detected on the ground. The amplitude and phase of VLF signals, after propagating for long distances inside the wave-guide defined by the base of ionosphere and the ground, depends on the electron conductivity and on the reflection height parameters (Wait & Spies 1964), respectively. The D-region (60 - 90km) is formed by the direct incidence of the solar Lyman-alpha radiation (Nicolet & Aikin 1960), and can be strongly disturbed during solar flares by the enhancement of the X-ray emission (McRae & Thomson 2004, Raulin et al. 2006, 2010). At night this region disappears, due to the lack of solar radiation and the higher recombination rate at lower altitudes, and so the base of ionosphere changes to about 90 km, which is the E-region that extends up to ~200 km

of height. In addition to ionizing radiation, the low ionosphere density can also be changed by energetic particle precipitation events from the radiation belts (Helliwell et al. 1973, Inan et al. 1982, Fernandez et al. 2003, Peter & Inan 2004, Fernandez & Correia 2013).

These physical parameters control the ionosphere refractive index (Wait & Spies 1964), which is impacted by changes in space weather events, and can be detected as VLF amplitude and/or phase variations. These variations are obtained when comparing the disturbed VLF daily profile with a quiet day profile.

Riometer

Riometer measurements started at EACF in 2009 using two 1-channel riometers at 30 and 38 MHz, with polarization measurements at 38 MHz. These riometers located in Antarctica are official stations that belong to the South America Riometer Network (SARINET - http://polaris.nipr.ac.jp/~ytanaka/riometer.html), which consists of 11 stations operating in South America inside an international collaboration among Brazil, Japan, Argentine and Chile.

The relative ionospheric opacity meter (riometer) is a radio receiver used to detect the background cosmic noise on the Earth´s surface after the signal has passed by the ionosphere. The receiver frequency is usually between 20 and 50 MHz, near the ionospheric cutoff frequency in the low ionosphere, where the collisions between the electrons and the constituents of the neutral atmosphere is high, and the radio wave is absorbed during electron density enhancements. This technique is based on a definition of a quiet day curve (QDC) obtained during periods of low solar and geomagnetic activity. The ionospheric disturbances are obtained from the logarithmic ratio between the QDC and the disturbed day curve, which gives the parameter called cosmic noise absorption (CNA). The ionosphere absorption occurs in the D- and E-regions (~90 - 100 km of height), mainly due to electron precipitation events, or in association with other phenomena that changes the collision frequency. The riometer can be a simple broad beam dipole antenna (>60°) called 1-channel riometer, or an array of dipole antennas of narrower beam called imaging riometer. The latter one is used for mapping 2-D spatial small-scale structures at ionospheric heights around 100 km.

Global navigation satellite systems (GNSS)

The GNSS receivers of dual frequency (L1: 1.575GHz and L2: 1.228GHz) are used for ionospheric soundings. The frequency dispersive property of the ionosphere produces differential phase shifts between the two radio signals after propagating through the ionosphere. These shifts are proportional to the total electron content (TEC), which is the electron concentration in the plasma column between the satellite and receiver. The TEC measurements are representative of the F-region conditions at ~300 km, where is the peak of ionospheric electron density. A JAVAD GPS receiver for ionospheric observations started to operate at EACF in 2004, recording RINEX (Receiver Independent Exchange Format) data with 15s time resolution. The vertical GPS-TEC (VTEC) is derived at each 30s from the RINEX data using the pre-processing stage of the local point interpolation method (LPIM) algorithm (Brunini et al. 2008), considering only satellites with elevation angle above 30° and assuming the ionospheric height of 350 km.

The ionospheric irregularities produce fast variations in the amplitude and phase of GNSS signals, called ionospheric scintillations, affecting the accuracy of GNSS measurements. The scintillation and TEC measurements at EACF started in 2010 using a GNSS Ionospheric Scintillation and Total Electron Content (TEC)

Monitor (GISTM). The GISTM system was conceived to investigate the ionospheric scintillations, particularly by the system of the GPS Silicon Valley (GSV), model GSV 4004B (Van Dierendonck et al. 1993), which is a NOVATEL OEM4 dual-frequency receiver that was developed to compute and record amplitude (S4) and phase (sigma-phi) scintillation indices with 60s time resolution, as well as the ionospheric TEC and its changes with 15s time resolution.

The ionospheric large spatial characterization of TEC and scintillation from Antarctica up to the Brazilian territory has been investigated by the data from the GNSS network of IBGE (Instituto Brasileiro de Geografia e Estatística, https://www.ibge.gov.br/). The mapping of the scintillation locations can be obtained using the GNSS network, which permits to characterize the spatial distribution of the ionospheric irregularities as function of its dynamics and space weather conditions. The methodology used to obtain the maps is the same as described by Spogli et al. (2009, 2013), which considers the percentage of scintillation occurrence above a defined threshold inside a bin of 3h MLT duration x 2^0 MLat.

Ionosonde

At EACF the ionospheric sounding using ionosonde started in 2009, when it was installed a Canadian Advanced Digital Ionosonde (CADI - MacDougall et al. 1993). The ionosonde data refer to vertical soundings done at each 5 min with frequencies between 1 and 20 MHz, which gives the virtual height where each frequency was reflected. The plot of the virtual height against the frequency is known as ionogram, and is used to obtain the ionospheric parameters foF2 (critical electron density) and hmF2 (height of electron density peak) of the F2 region as a function of frequency. The ionosonde parameters are obtained using the 'UNIVAP Ionosonde Digital Data Analysis' (UDIDA, Pillat et al. 2013) tool that manually permits to analyze the ionograms recorded by CADI. The ionograms can also give information about ionospheric irregularities, which can be identified in fuzzy ionograms, and, in extreme cases, in the loss of signal.

The ionosonde database obtained at EACF are complemented by data from national and international ionosonde networks operating in South America and Antarctica, which are available in the sites *Estudo e Monitoramento BRAsileiro de Clima Espacial* (EMBRACE/INPE, http://www2.inpe.br/climaespacial/portal/en/) and Australian World Data Center (https://www.sws.bom.gov.au/World_Data_Centre).

RESULTS

The investigations at EACF in the last two decades have been performed to characterize the ionospheric behavior at different time scales, from long term associated with the 11-year solar cycle to shorter periods associated with seasonal, atmospheric phenomena and space weather, as well as the connection of the ionosphere with the dynamics from high to lower latitudes in the South America sector.

Ionospheric behavior versus solar radiation

The long term investigations using ionospheric VLF sounding at EACF were done with the continuous measurements of the VLF amplitude in the NPM-EACF path from 2003 to 2008 using Stanford MSK receiver, covering the maximum and decay phase of the 23rd solar cycle (Correia et al. 2011), and using measurements in the NPM-EACF, NAA-EACF, NPM-ROI and NAA-ROI paths from 2007 to 2011 (Correia et al. 2013a), making use of AWESOME receiver, covering the minimum of 23rd and increasing phase of the 24th solar cycles. In both works, the mid-day VLF amplitude

showed clearly a slow trend variation associated with solar Lyman-alpha radiation evolution during solar cycle (Figure 1), as expected since it is affected by the conductivity at the D-region, and this is controlled by the ionizing radiation (Nicolet & Aikin 1960). These results reinforced the solar radiation control of the low ionosphere, which were previously suggested

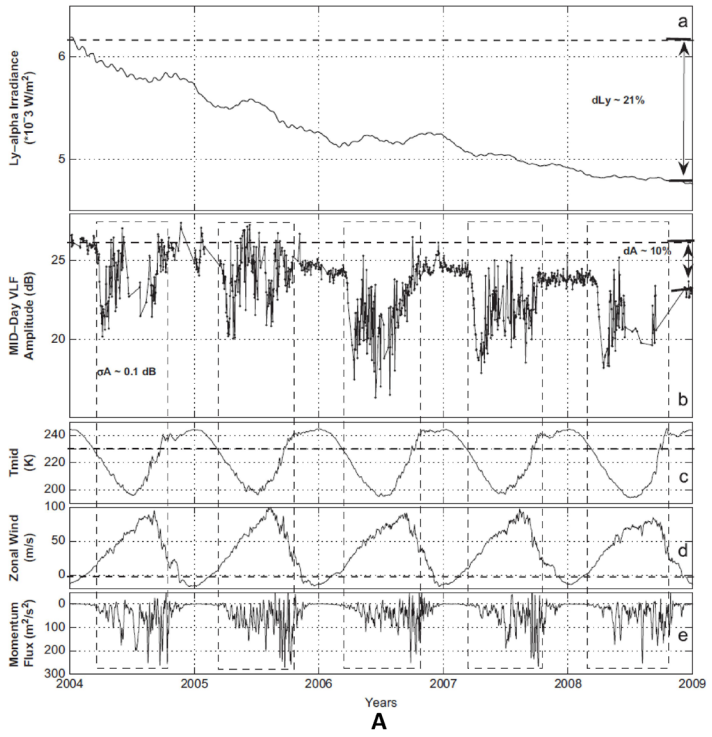

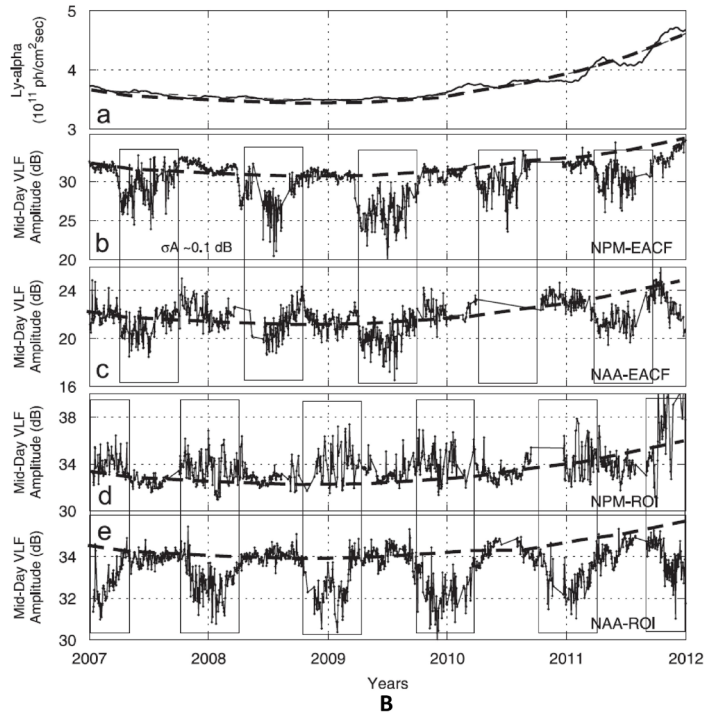

Figure 1. Comparison of daily mid-day VLF amplitude with the 27-day smoothed solar Lyman-alpha radiation (top panel) during the decay phase of 23rd solar cycle (A), and 23rd minimum and the increase of the 24th solar cycle (B). (A) top to bottom: (a) solar radiation, (b) VLF signal from NPM-EACF path, and (c) the stratospheric parameters temperature, (d) zonal wind velocity and (e) momentum flux measured at southern mid-latitudes (Figure adapted from Correia et al. 2011). (B) top to bottom: (a) solar radiation, VLF signals from (b) NPM-EACF, (c) NAA-EACF, (d) NPM-ROI and (e) NAA-ROI paths (Figure adapted from Correia et al. 2013a).

from studies of solar flare impact in the D-region detected as sudden phase anomalies (SPAs) of the VLF signals (Pacini & Raulin 2006, Raulin et al. 2006). The SPAs studies showed that during solar minimum, even weak solar X-ray flares can disturb the ionosphere, showing that the ionospheric sensitivity is higher in this period (Pacini & Raulin 2006, Raulin et al. 2006, 2010, Macotela et al. 2017).

The effect of solar radiation in the ionosphere from GPS-TEC measurements at EACF was done comparing the daytime maximum VTEC, which was the median VTEC values obtained between 15:00 UT and 17:00 UT (~14 LT) from 2004 to 2011 (Correia et al. 2013b), with the 30.4 nm ultraviolet radiation (FUV) used as solar proxy (Figure 2). The FUV is the spectral solar irradiance of the He II emission measured with TIMED SEE (Thermosphere Ionosphere Mesosphere Energetics and Dynamics – Solar Extreme Ultraviolet [EUV] Experiment), which data are available at the Solar Irradiance Data Center of the Laboratory for Atmospheric and Space Physics (LASP) (http://lasp.colorado.edu/lisird/lya/) (Woods et al. 2000).

Figure 2 clearly shows a good correlation between the 31-day smoothed data of daytime maximum VTEC and FUV, with both presenting a slow temporal variation well fitted by a third-degree polynomial (dashed lines), associated with the 11-year solar cycle.

The long-term investigations of the ionosphere behavior at EACF using VLF and GPS-TEC measurements show clearly the 11-year solar cycle modulation; and particularly in the GPS-TEC measurements show a dependence on the solar zenith angle, which is less evident during the winter seasons at high latitude when the Sun is mostly below the horizon (Correia et al. 2013b).

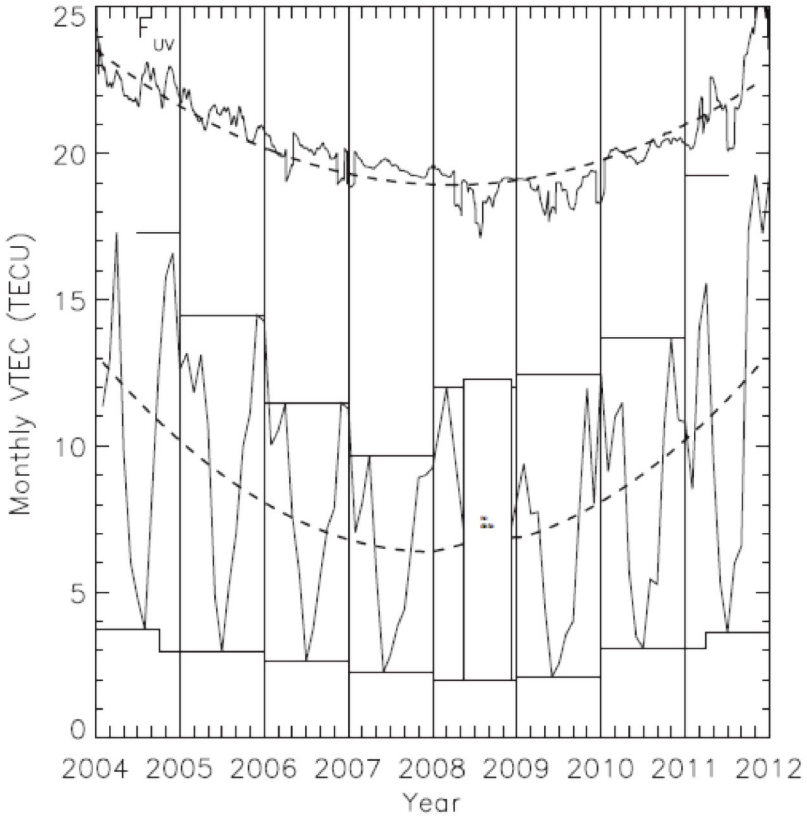

Figure 2. Comparison of the monthly averaged daytime maximum VTEC (lower curve) with the 31-day smoothed solar He II radiation (30.4 nm, FUV) (top curve) from 2004 to 2011. The wrapping of the VTEC is the yearly maximum and minimum values. The dashed lines refer to a third-degree polynomial fitting. (Figure adapted from Correia et al. 2013b).

Climatology of ionospheric irregularities

The ionospheric irregularity investigations have increased our understanding of their variations associated with solar cycle, season and geomagnetic conditions, but it is still difficult to predict the occurrence of irregularities, because the ionosphere is very dynamic even during quiet geomagnetic periods. The ionospheric electric fields at low latitudes are generated by the action of the thermospheric neutral winds, which drives the equatorial vertical plasma drifts (e.g., Fejer 1997). The daytime upward vertical drifts produce a field-aligned plasma diffusion from equator to higher latitudes, which is responsible by the equatorial ionization anomaly (EIA). The EIA is characterized by ionospheric plasma redistribution with lower density near equator, and higher density at two symmetric regions located at magnetic latitudes of ~±15°, the so called EIA crests. The EIA crests are intensified and displaced to higher latitudes during the first hours of the main phase of geomagnetic storm due to the action of the daytime prompt penetration electric field (PPEF, Tsurutani et al. 2004), but later on they can be strongly affected by the thermospheric winds originated at high latitudes due the auroral heating, which produce disturbance dynamo electric fields (DDEF), and become dominant at low latitudes (e.g., Abdu et al. 2012). Ionospheric irregularities at low latitudes occur in close association with the EIA crests and appear mostly after post-sunset hours, when there is a pre-reversal enhancement of the vertical upward drift, and are more intense at the bottom of the equatorial ionosphere (Balan et al. 2018), while at high latitudes they occur more frequently inside the auroral region.

The ionospheric irregularities have been observed as GNSS scintillations, and are highly dependent on magnetic local time, geographic location, geomagnetic activity, season of the year, and solar cycle (e.g., de Franceschi et al. 2008, Spogli et al. 2009, 2013, Thomas et al. 2013, Prikryl et al. 2016, Muella et al. 2017, Correia et al. 2017, 2018, and references therein).

Ionospheric scintillation climatology in the South America has been improved after using GNSS receivers´ networks. An investigation of ionospheric scintillation from Latin America to Antarctica identified areas with enhanced probability of scintillation occurrence, called of hot-spots (Spogli et al. 2013). Figure 3 shows the map of the percentage of scintillation occurrence with SigmaPhi index above 0.1 treshold, where are identified the hot-spots, which are associated with post-sunset (PST) hours and South America Magnetic Anomaly (SAMA) at low latitudes, and daytime magnetic cusp (CUSP), magnetotail region (TAIL) and polar cap patches (PATC) at high latitudes.

The scintillation activity also has association with geomagnetic storms, at low latitudes the ionospheric scintillations can be suppressed when the main phase storm is during daytime well before the sunset, and they can also be triggered or intensified when the main phase storm occurs before or near post-sunset hours (e.g., de Paula et al. 2019). At mid- and high-latitudes strong ionospheric scintillations were observed during the moderate geomagnetic storm occurred on 26-27 September 2011, particularly they appeared on the dayside during the initial phase storm in association with transpolar Sun-aligned arcs, and during the main phase in the location of storm enhanced density (SED) plumes at mid-latitudes and cusp; they also appeared in the auroral oval region, and in association with tongues of ionization (TOI) structures observed inside the polar cap on the nightside (Correia et al. 2017).

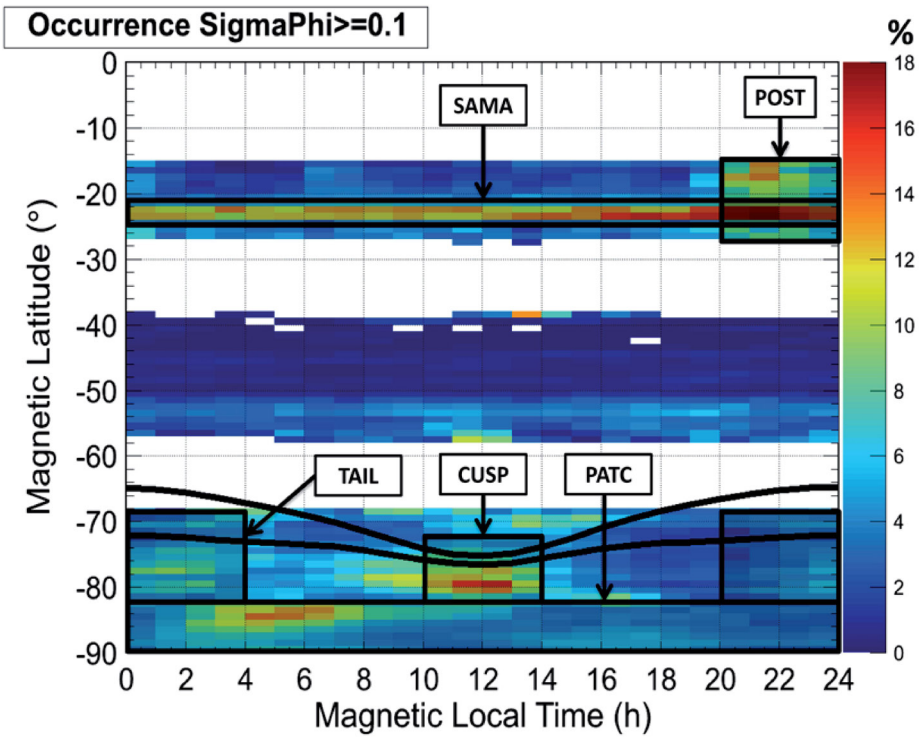

Figure 3. Map of SigmaPhi percentage of scintillation occurrence above the threshold of 0.1 radians. The black curve is the modeled Feldstein oval for magnetic quiet condition, and the black boxes define the ionospheric hot-spots. (Figure adapted from Spogli et al. 2013).

Ionosphere behavior versus neutral atmosphere dynamics

The mid-day VLF amplitude analysis also presented strong variations (Figure 1) from April to September in the NPM- and NAA- EACF paths that are mostly located in the southern hemisphere, and from November to March in the NPM- and NAA-ROI paths that are mostly located in the northern hemisphere. Thus, these stronger variations occurred during the wintertime in the hemisphere the respective VLF paths were mostly located, so they were attributed to meteorological processes and phenomena, which affected the lower ionosphere (Correia et al. 2011, 2013a). These VLF fluctuations presented a strong 16-day period, which was present in the stratospheric temperature measurements done over EACF by SABER experiment (Correia et al. 2011), and in the meteor radar measurements of the mesosphere and lower thermospheric physical parameters done at Rothera (a British Antarctic Survey Station) during the same years as reported by Day & Mitchell (2010) So, these 16-day VLF fluctuations were attributed to the effect of the planetary waves propagating upwards after being generated in the neutral atmosphere, and gives the evidence of vertical couplings among all atmospheric layers.

The atmospheric couplings were reinforced from the investigation of gravity waves (GWs) at the lower ionosphere. The GWs can modulate the neutral atmosphere and generate fluctuations in the electrical conductivity at the low ionosphere, which can be detected as VLF amplitude variations. The GW events are characterized by the period and time duration parameters obtained from the VLF amplitude using wavelet spectral analysis (Correia et al. 2020). Figure 4 shows an example of one GW event detected at EACF on 10 July 2007 using VLF technique. The GW event is visible as stronger amplitude fluctuations between 01:30 and 03:00 UT (Figure 4a), and identified as orange color in the wavelet power spectra (Figure 4b), with wave period between 8 and 16 min (Figure 4c). This

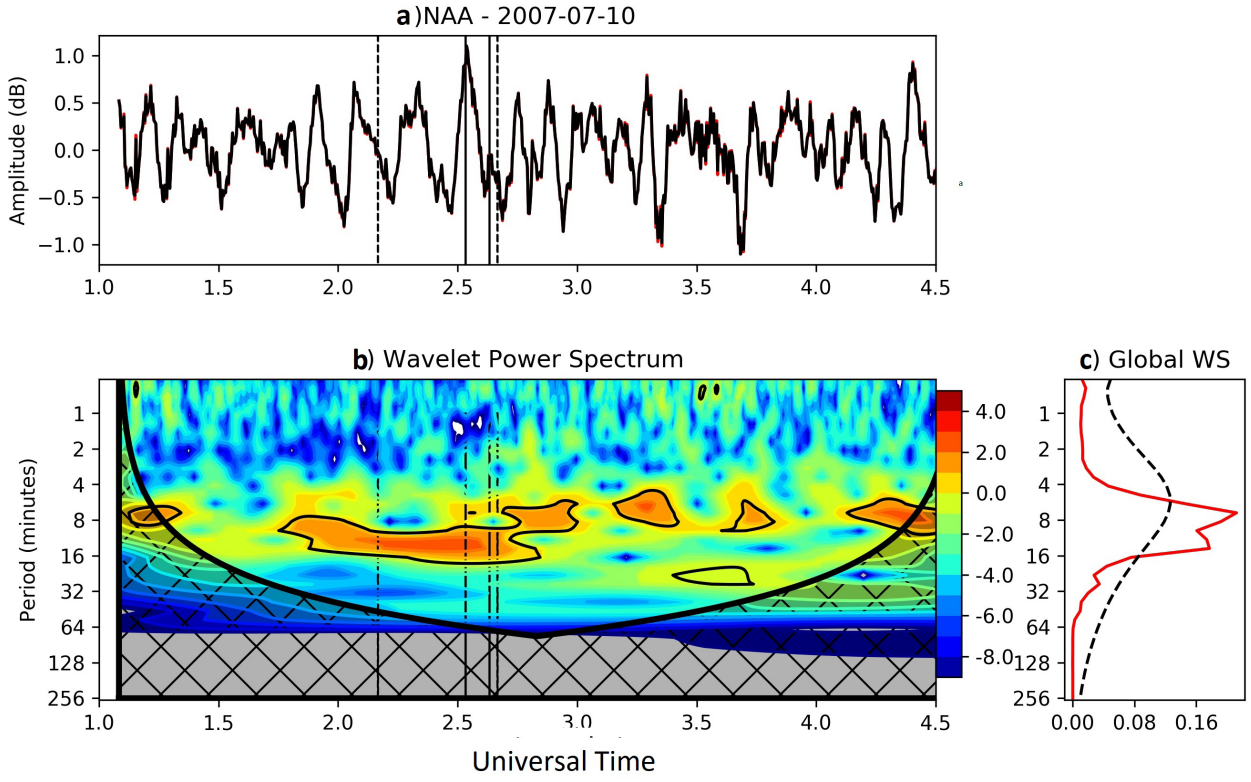

Figure 4. Wavelet spectral analysis of the VLF signal amplitude detected at EACF on 10 July 2007. (a) The residual VLF amplitude after subtracting a 10-min running mean. (b) Wavelet power spectra, with regions of confidence levels greater than 95% (inside black contours), and the cross-hatched areas where edge effects are important. (c) Time-averaged wavelet power spectra (Global WS). (Figure adapted from Correia et al. 2020).

GW event was observed simultaneously with a co-located airglow imager operating at EACF (Bageston et al. 2011).

Correia et al. (2020) also investigated the occurrence of GW events at EACF using the VLF technique during all the year of 2007. The statistical study of the GW events showed they occur all year round, but showing distinct characteristics between night and day occurrences (Figure 5). The nighttime GW events presented periods mostly between 5 and 10 min (red bars) occurring in higher number during winter season with the maximum in August, while daytime events had wave periods mostly below 5 min (blue bars), and these occurred in higher number and dominated all days of the months from November to April.

Ionosphere versus space weather

The ionosphere is strongly affected by space weather conditions, mainly during geomagnetic storms, but also by solar proton events (SEPs) and relativistic electron precipitation events, which can precipitate deeper in the atmosphere at middle and high latitudes. In the following we present the main results obtained in this context.

The compression of the Earth's magnetosphere, under the impact of CMEs and solar high-speed streams (HSS) causing geomagnetic storms, induces strong electric fields and increases the magnetosphere convection, which can strongly affect the ionosphere dynamics. During few hours just after the onset of geomagnetic storms, the

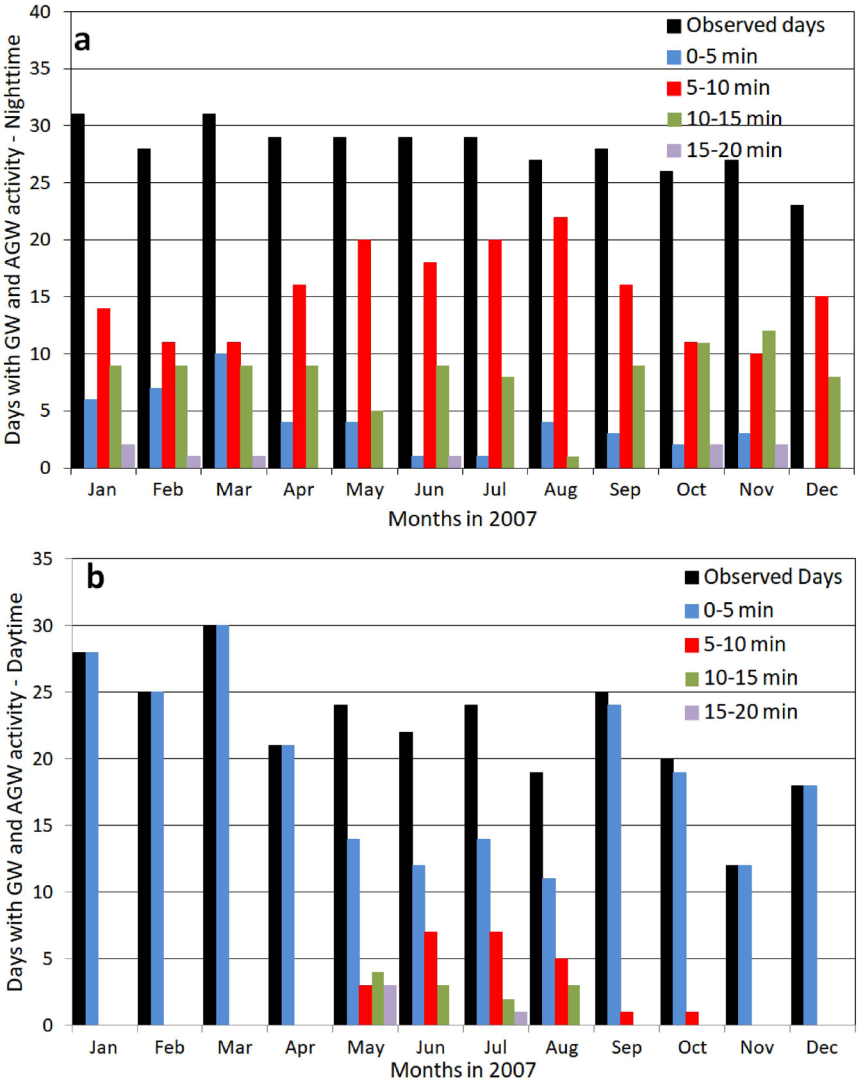

Figure 5. Monthly GW events detected at EACF on 2007 using VLF technique separated in night (a) and day (b) hours. The black bars give the observed days per month. The colored bar gives the monthly number of observed GWs with predominant period in the following intervals: 0–5 (blue), 5–10 (red), 10–15 (green), and 15–20 min (purple). (Figure adapted from Correia et al. 2020).

PPEF is dominant (e.g., Tsurutani et al. 2008), and operates at equatorial latitudes affecting the ionosphere dynamics, intensifying the fountain effect in the dayside, and lifting the equatorial plasma to higher altitudes and latitudes, while downwards the plasma in the nightside. At high latitudes, the precipitation of energetic particles in the thermosphere increases the electrical currents in the auroral zone, which are dissipated by the Joule effect and heats the plasma that expands, changing the thermosphere composition and the neutral winds circulation (e.g., Danilov & Lastovicka 2001), which are reinforced by the disturbance dynamo electric field (DDEF). During strong geomagnetic storms the combination of these processes are responsible by large-scale ionospheric plasma redistribution from equatorial to polar latitudes.

The ionospheric response to moderate-strong geomagnetic storms from equatorial to high latitudes using multi-instruments operating in the Antarctica and South American sectors permitted the characterization of the ionosphere dynamics as a function of storm time and magnetic local time.

The impact of the 26 September 2011 geomagnetic storm in the ionosphere was investigated from middle to high latitude

considering stations (Table I) in the Antarctica American and Australian sectors (Correia et al. 2017). This study permitted the evaluation of the PPEFs role in the ionospheric storm-enhanced densities (SED) at mid-latitudes and in the tongues of ionization (TOIs) at polar latitudes. The analysis compared the disturbed days with a QDC, which was obtained by considering the averaging of the nearest four quiet geomagnetic days, which means Kp < 2 and AE < 200 nT. The ionospheric conditions were obtained using GPS-TEC in TEC units (1 TECU = 10^{16} el m^{-2}), and NmF2 obtained from the ionosonde parameter foF2 by using the relation NmF2 = 1.24 x (foF2 in MHz)^2 x 10^{10} in 10^{11} el m^{-3} units. Figure 6 shows GPS-TEC and NmF2 increases associated with SEDs during the main phase of the geomagnetic storm –in the dayside (American sector, Figure 6a) at mid-latitudes, while shows density depletions in the nightside (Australian sector, Figure 6b) from middle to high latitudes. The goal of this study was to characterize the SED and TOIs formation during the geomagnetic storm taking into account the PPEF effect. The dayside SED was observed at mid-latitudes just in the beginning of main phase storm suggesting it was formed under the PPEF effect. The TOI formation occurred when the SED plumes were near the dayside cusp, from where the SED plasma could reach the nightside polar cap. Strong GNSS scintillations were observed in close association with mid-latitude SED and cusp structures on the dayside, and polar cap TOI on the nightside.

The 22-23 June 2015 geomagnetic storm was investigated using VTEC measurements and NmF2 parameter done at different station locations from equatorial to high latitudes (Table II) in the South America sector (Macho et al. 2020). The geomagnetic storm started in the local afternoon, and during the first hours of its main phase, increases of VTEC were observed at almost all stations (Figure 7a), while NmF2 (Figure 7b) showed increases at mid- high-latitude stations and decreases at low and equatorial stations. This daytime ionospheric response is expected when it is under the PPEF effect (e.g., Tsurutani et al. 2008, Correia et al. 2017), which uplifts the plasma at the equator increasing the electron density at higher altitudes and moves the EIA crest to higher latitudes. This initial large-scale plasma redistribution was followed by VTEC and NmF2 variations suggesting plasma propagation from high to mid-latitudes under the dusk effect in the F-region (Buonsanto

Table I. Station names with respective geographic and geomagnetic coordinates, and instrumentation.

Station Name	Geographic coordinates		Geomagnetic coordinates		LT	MLT Mid$^+$	instrument list
	Lat (°N)	Long (°E)	Lat (°N)	Long (°E)		UT	
American Sector							
Port Stanley (PST)	-51.70	-57.89	-37.63	10.55	UT-4	4	iono
Comandante Ferraz (EACF)	-62.08	-58.39	-47.11	11.73	UT-4	4	GNSS, iono
San Martin Base (SMA)	-68.13	-67.10	-52.66	8.32	UT-4	4	iono
Australian Sector							
Hobart (HOB)	-42.88	147.35	-54.12	-133.45	UT+10	13	iono
Macquire Island (MCI)	-54.50	158.95	-64.54	-111.90	UT+10	12	iono
Mario Zucchelli Station (BTN)	-74.70	164.12	-80.00	-52.45	UT+12	8	GNSS
Concordia Station (DMC)	-75.25	124.17	-88.68	43.26	UT+8	1	GNSS

1999), when DDEF process became dominant. After sunset, almost in the end of main phase storm, ionospheric disturbances were observed in the E-region at stations located inside SAMA suggesting episodes of particle precipitation.

In addition to the impact of geomagnetic storms, SEP events can also disturb the ionosphere at middle and high latitudes (e.g., Lastovicka 2009). The investigation of the ionosphere in Antarctica and at lower latitudes in the South America, under the impact of two SPE events that occurred on 23 and 27 January 2012, showed that it was strongly disturbed by GeV protons (Correia et al. 2013c). This conclusion was achieved by the ionospheric absorption detected by riometers and VLF receivers at mid-latitudes in the South America and at high latitudes in Antarctica, and it was reinforced by significant cosmic rays increases detected during the same events with CARPET experiment (Makhmutov et al. 2013) at location with rigidity near 10 GV in South America, evidencing > 10 GeV protons.

Localized plasma density disturbances also have been identified in the low ionosphere from VLF measurements done during the night. These small and localized disturbances are detected as fast temporal variations of the amplitude and phase of VLF signals, when the ionosphere is not saturated by the solar radiation, and are known as Trimpi events. The plasma disturbances are caused by secondary ionization in the D-region produced by electron precipitation events from the Van Allen radiation belts (Helliwell et al. 1973), and have been mostly attributed to resonant interactions with whistler waves generated by lightnings (e.g., Helliwell et al. 1973, Inan et al. 1978, Inan & Carpenter 1987). Statistical studies of Trimpi events detected at EACF have shown they occur preferentially near the equinoxes, in close association with geomagnetic active periods (Fernandez et al. 2003), occurring in higher number during the recovery phase of some geomagnetic storms, and also in close association with flux enhancements of the high energy electrons in the radiation belts (Fernandez & Correia 2013). Fernandez & Correia (2013), based on these results, suggested the occurrence of Trimpi events is a function of the electron population of radiation belts, the wave-particle interaction possibility (i.e., ideal pitch angle conditions) and the availability of interacting waves, which can be the whistler-waves generated by lightning, or the chorus and electromagnetic ion cyclotron (EMIC) waves generated in the magnetosphere.

The monitoring of the lower ionosphere using VLF technique during nighttime also showed the possibility of VLF to be used to study nonsolar transients, as the outbursts from astrophysical objects like soft gamma ray repeaters (SGRs). The AWESOME VLF measurements obtained with few ms time resolution permitted the detection of the ionospheric response to the X-ray bursts from SGR J1550-5418 occurred on 22 January 2009 (Raulin et al. 2014). The detection of SGRs using VLF is rare, this is one of the four cases of SGRs detected using VLF reported in the literature. Figure 8 shows an example of a sequence of X-ray bursts of the SGR object detected by ACS/SPI (http://www.isdc.unige.ch/integral/science/grb#ACS) instrument that measures the integral X-ray counts with 50 ms time resolution, with almost all of them associated with VLF amplitude decreases, most evident at longer NPM-EACF VLF path. Raulin et al. (2014) found out that the illumination extension of the VLF propagation path by the flaring object is very important, because it defines the VLF sensitivity threshold to detect the X-ray burst emission from nonsolar transients.

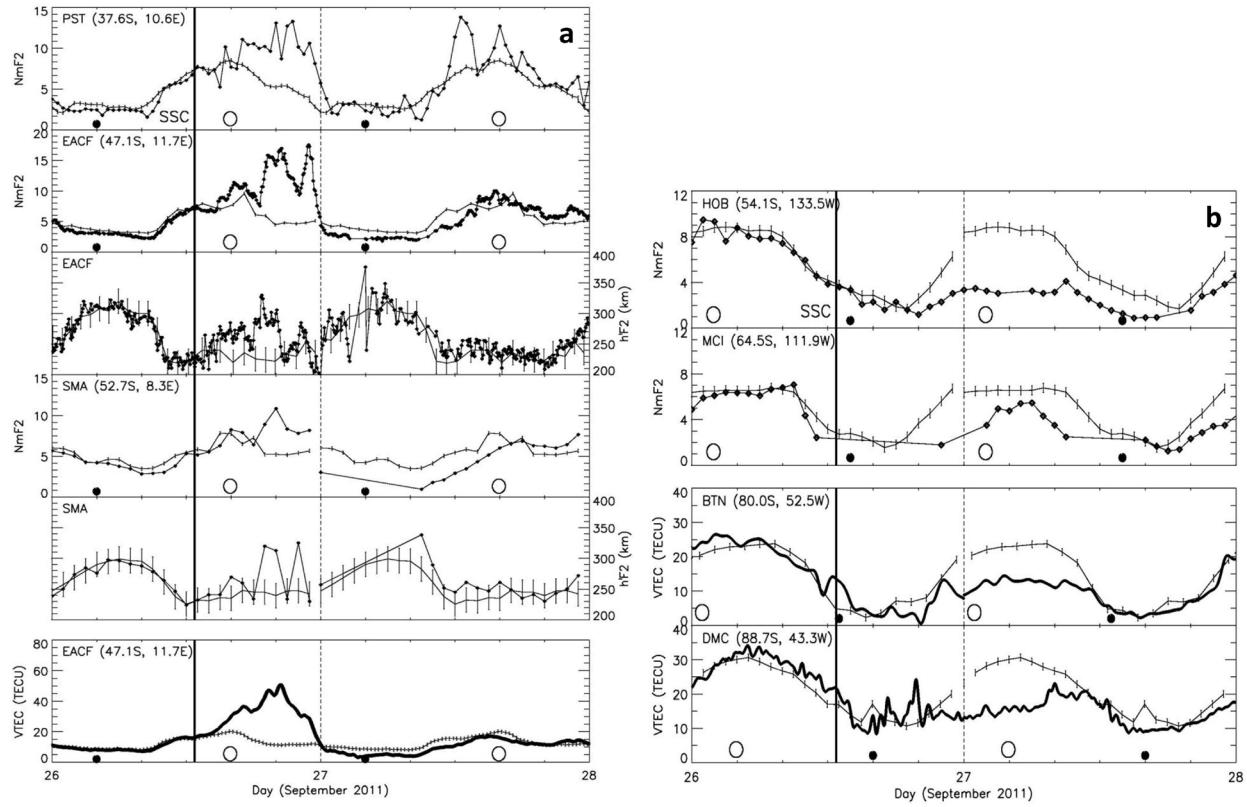

Figure 6. VTEC and NmF2 variations in the Antarctica (a) American and (b) Australian sectors during the 26-27 September 2011 geomagnetic storm (dotted/line darker curves) compared with the quiet day curve (QDC, light curves). The labels on the panels refers to station names and respective geomagnetic coordinates. NmF2 is in 10^{11} el m^{-3} units. The error bars on QDC curves are the standard deviation (± s) of the respective parameter. The horizontal arrow identifies the main phase of magnetic storm. (Figure adapted from Correia et al. 2017).

Table II. Station names with respective instrumentation, geographic coordinates and dip angle.

Station Name	GNSS	Ionosonde	Latitude	Longitude	dip angle
Boa Vista (BOA)	X	X	02.8 N	060.7 W	18.6 N
Jicamarca (JIC)		X	12.0 S	076.9 W	00.0 S
Belém (BEL)	X		01.5 S	048.4 W	01.6 S
São Luis (SLU)		X	02.6 S	044.2 W	08.9 S
Arequipa (ARE)	X		16.5 S	071.5 W	09.1 S
Cuiabá (CUI)	X		15.6 S	056.1 W	17.6 S
Fortaleza (FOR)	X	X	03.7 S	038.5 W	17.7 S
Campo Grande (CGR)	X	X	20.4 S	054.5 W	26.1 S
Cachoeira Paulista (CHP)	X	X	22.7 S	045.0 W	37.5 S
Porto Alegre (POA)	X		30.1 S	051.1 W	39.7 S
Port Stanley (PST)	X	X	51.6 S	058.0 W	49.8 S
Estação Comte Ferraz (ECF)	X		62.1 S	058.4 W	55.5 S
Rothera Station (ROT)	X		67.6 S	068.1 W	59.4 S

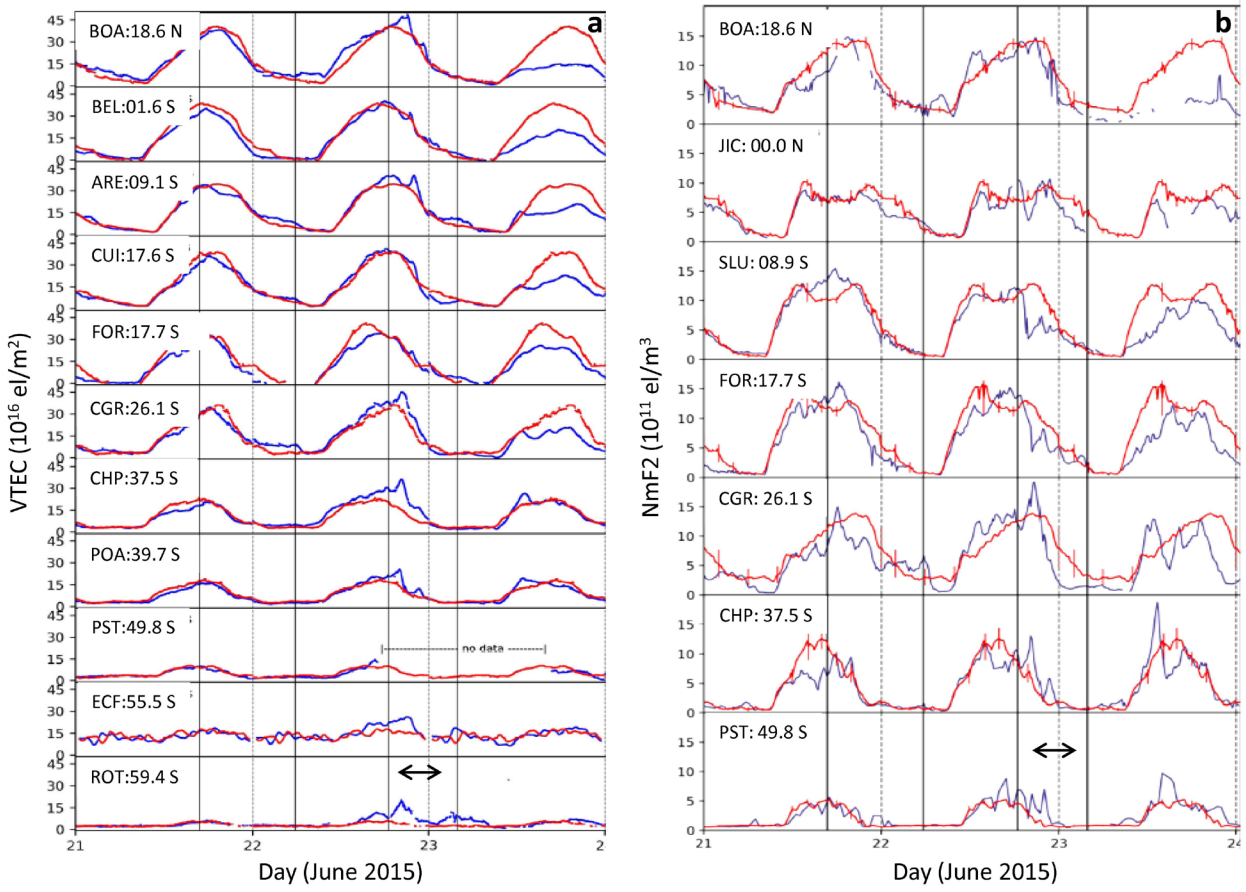

Figure 7. VTEC (a) and NmF2 parameter (b) variations (blue lines) from 21 to 25 June 2015 compared with QDC curves (red lines) at different latitudes in the South America sector. The labels on the panels refers to station names and respective dip angles. The horizontal arrow identifies the main phase of the intense geomagnetic storm. (Figure adapted from Macho et al. 2020).

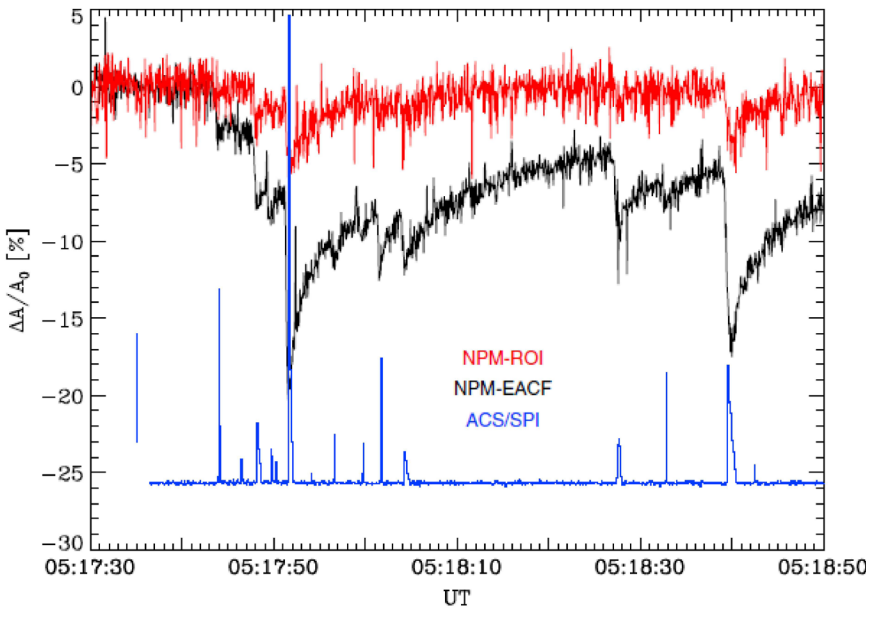

Figure 8. Example of VLF amplitude decreases observed at EACF (black curve) and at ROI (red curve) associated with a sequence of X-ray bursts (blue curve) of the SGR J1550-5418 detected with ACS/SPI instrument. The blue vertical line on the left refers an ACS/SPI count rate of 2 x 10^5 counts/s. (Figure adapted from Raulin et al. 2014).

CONCLUSION

This work presented the main scientific results of the ionospheric investigations done at EACF in the last few decades. The investigations show that the ionosphere presents variations in time scales ranging from years to few ms timescales under the solar and astrophysics phenomena from outside and of atmospheric origin from below. The characterization of the quiet and disturbed ionosphere is scientifically important, but nowadays it is also of great interest of the actual technologic society, which widely uses radio communication and navigation systems. The ionospheric disturbances are problem for the users of GNSS navigation systems, HF communication, and are critical for satellite control systems, stabilization of petrol platforms, air navigation and precision agriculture. So, understanding the ionospheric climatology as a function of space weather conditions is highly essential to define its spatial distribution and time of occurrence.

Acknowledgments

EC thanks the Conselho Nacional de Desenvolvimento Científico e Tecnológico (CNPq, Brazil, nos.: 406690/2013-8, 442101/2018-0 and 306818/2019-1), Fundação de Amparo à Pesquisa do Estado de São Paulo (FAPESP, Brazil, no.: 2019/05455-2) for individual research support, and the Instituto Nacional de Pesquisas Espaciais (INPE/MCTI). The INCT-APA (Instituto Nacional de Ciência e Tecnologia Antártico de Pesquisas Ambientais, CNPq proc.574018/2008-5 and Fundação de Amparo à Pesquisa do Estado do Rio de Janeiro - FAPERJ proc. E-16/170.023/2008). The authors also acknowledge the support of the Ministério da Ciência, Tecnologia e Inovações (MCTI); Ministério do Meio Ambiente (MMA); and Comissão Interministerial para os Recursos do Mar (CIRM) for supporting the Antarctic activities. These studies are part of the activities inside the GRAPE Expert group (www.grape.scar.org), endorsed by SCAR to facilitate the collaboration (http://www.grape.scar.org/). The GNSS data from the DMC and BTN Italian Stations were obtained in the framework of the Programma Nazionale di Ricerche in Antartide (PNRA, Italian National Program for Antarctic Research). Ionosonde data from the Argentinean San Martin Station were available upon request from Adriana Gulisano (adrianagulisano@gmail.com) from the Argentine Antarctic Institute. The GNSS data were obtained in the International GNSS Service (IGS) and Brazilian Continuous Monitoring Network (RBMC). The ionosonde data were obtained from UK Solar System Data Center (UKSSDC - http://www.ukssdc.ac.uk) and from Brazilian Studies and Monitoring of Space Weather (EMBRACE - http://www.inpe.br/climaespacial/SWMonitorUser). EPM and LTMR thank the Coordenação de Aperfeiçoamento de Pessoal de Nível Superior Brasil (CAPES, Brazil) for the financial support providing scholarship through Financial Code 001.

REFERENCES

ABDU MA, BATISTA IS, BERTONI F, REINISCH BW, KHERANI EA & SOBRAL JHA. 2012. Equatorial ionosphere responses to two magnetic storms of moderate intensity from conjugate point observations in Brazil. J Geophys Res 117: A05321. doi:10.1029/2011JA017174.

BAGESTON JV, WRASSE CM, BATISTA PP, HIBBINS RE, FRITTS DC, GOBBI D & ANDRIOLI VF. 2011. Observation of a mesospheric front in a thermal-doppler duct over King George Island, Antarctica. Atmos Chem Phys 11: 12137-12147. doi: 10.5194/acp-11-12137-2011.

BALAN N, LIU L & LE H. 2018. A brief review of equatorial ionization anomaly and ionospheric irregularities. Earth and Planetary Physics 2: 257-275. doi: 10.26464/epp2018025.

BRUNINI C, MEZA A, GENDE M & AZPILICUETA F. 2008. South American regional ionospheric maps computed by GESA: a pilot service in the framework of SIRGAS. Adv Space Res 42: 737-744. doi:10.1016/j.asr.2007.08.041.

BUONSANTO MJ. 1999. Ionospheric storms – a review. Space Sci Rev 88: 563-601.

COHEN MB, INAN US & PASCHAL EW. 2010. Sensitive broadband ELF/VLF radio reception with the AWESOME instrument. IEEE Trans Geosc Remote Sensing 48(1): 3-17. doi:10.1109/TGRS.2009.2028334.

CORREIA E, KAUFMANN P, RAULIN JP, BERTONI FC & GAVILÁN HR. 2011. Analysis of daytime ionosphere behavior between 2004 and 2008 in Antarctica. J Atmos Terr Phys 73: 2272-2278. doi: 10.1016/j.jastp.2011.06.008.

CORREIA E, MAKHMUTOV VS, RAULIN JP & MAKITA K. 2013c. Mid- and low-latitude response of the lower ionosphere to solar proton events on January 2012. J of Phys Conf Ser (Online) 409: 1/012186-4. doi: 10.1088/1742-6596/409/1/012186.

CORREIA E, MUELLA MTAH, ALFONSI L, PROL FS & CAMARGO PO. 2018. GPS Scintillations and Total Electron Content Climatology in the Southern American Sector. In: Sanli DU (Ed), Accuracy of GNSS Methods, Turkey: IntechOpen, Turkey. doi: 10.5772/intechopen.79218.

CORREIA E, PAZ AJ & GENDE MA. 2013b. Characterization of GPS total electron content (GPS-TEC) in Antarctica from 2004 to 2011. Annals of Geophysics 56: R0217-1-R0217-5. doi: 10.4401/ag-6223.

CORREIA E, RAULIN JP, KAUFMANN P, BERTONI FC & QUEVEDO MT. 2013a. Inter-hemispheric analysis of daytime low ionosphere behavior from 2007 to 2011. J Atmos Terr Phys 92: 51-58. doi: 10.1016/j.jastp.2012.09.006.

CORREIA E, RAUNHEITTE LTM, BAGESTON JV & DAMICO DE. 2020. Characterization of gravity waves in the lower ionosphere using very low frequency observations at Comandante Ferraz Brazilian Antarctic Station. Ann Geophys 38: 385-394. doi:10.5194/angeo-38-385-2020.

CORREIA E, SPOGLI L, ALFONSI L, CESARONI C, GULISANO AM, THOMAS EG, RAMIREZ RFH & RODEL AA. 2017. Ionospheric F-region response to the 26 September 2011 geomagnetic storm in the Antarctica American and Australian sectors. Ann Geophys 35: 1113-1129. doi: 10.5194/angeo-35-1113-2017.

DANILOV AD & LASTOVICKA J. 2001. Effects of geomagnetic storms on the ionosphere and atmosphere. Int J Geomagnetic Aeronomy 2: 209-224.

DAY KA & MITCHELL NJ. 2010. The 16-day wave in the Arctic and Antarctic mesosphere and lower thermosphere. Atmos Chem Phys 10: 1461-1472. doi: 10.5194/acp-10-1461-2010.

DE FRANCESCHI G, ALFONSI L, ROMANO V, AQUINO MHO, DODSON A, MITCHELL CN & WERNIK AW. 2008. Dynamics of high latitude patches and associated small scale irregularities. J Atmos Terr Phys 70: 879-888. doi: 10.1016/j.jastp.2007.05.018.

DE PAULA ER ET AL. 2019. Ionospheric irregularity behavior during the September 6–10, 2017 magnetic storm over Brazilian equatorial–low latitudes. Earth Planets Space 71: 42. doi: 10.1186/s40623-019-1020-z.

FEJER BG. 1997. The electrodynamics of the low-latitude ionosphere: Recent results and future challenges. J Atmos Terr Phys 59: 1465-1482. doi:10.1016/S1364-6826(96)00149-6.

FERNANDEZ JH & CORREIA E. 2013. Electron precipitation events in the lower ionosphere and the geospace conditions. Ann Geophys 56(2): R0218. doi: 10.4401/ag-6242.

FERNANDEZ JH, RIZZO PIAZZA L & KAUFMANN P. 2003. Trimpi occurrence and geomagnetic activity: Analysis of events detected at Comandante Ferraz Brazilian Antarctic Station (L= 2.25). J Geophys Res 108(A1): SIA10-SIA17. doi: 10.1029/2001JA009213.

HEELIS RA. 2004. Electrodynamics in the low and middle latitude ionosphere: A tutorial. J Atmos Terr Phys 66: 825-838. doi: 10.1016/j.jastp.2004.01.034.

HELLIWELL RA, KATSUFRAKIS JP & TRIMPI ML. 1973. Whistler-induced Amplitude perturbation in VLF propagation. J Geophys Res 78: 4679-4688. doi: 10.1029/JA078i022p04679.

INAN US, BELL TF & CHANG HC. 1982. Particle precipitation induced by short-duration VLF waves in the magnetosphere. J Geophys Res 87: 6243-6264. doi: 10.1029/JA087iA08p06243.

INAN US, BELL TF & HELLIWELL RA. 1978. Nonlinear pitch angle scattering of energetic electrons by coherent VLF waves in the magnetosphere. J Geophys Res 83: 3235-3253. https://doi.org/10.1029/JA083iA07p03235.

INAN US & CARPENTER DL. 1987. Lightning-induced electron precipitation events observed at L ~ 2.4 as phase and amplitude perturbations on subionospheric VLF signals. J Geophys Res 92: 3293-3303. https://doi.org/10.1029/JA092iA04p03293.

JOHNSON MP, INAN US & LAUBEN DS. 1999. Subionospheric VLF signatures of oblique (nonducted) whistler-induced precipitation. Geophys Res Lett 26: 3569-3572. doi: 10.1029/1999GL010706.

LASTOVICKA J. 2006. Forcing of the ionosphere by waves from below. J Atmos Terr Phys 68: 479-497. doi: 10.1016/j.jastp.2005.01.018.

LASTOVICKA J. 2009. Lower ionosphere response to external forcing: A brief review. Adv Space Res 43(1): 1-14. doi: 10.1016/j.asr.2008.10.001.

MACDOUGALL JW, GRANT IF & SHEN X. 1993. The Canadian Advanced Digital Ionosonde: Design and Results. In: URSI GENERAL ASSEMBLY, Kyoto. Proceedings of UAG-104 Ionosondes and Ionosondes Networks, Kyoto: P. Wilkinson. https://www.ursi.org/files/CommissionWebsites/INAG/uag-104/index.html.

MACHO EP, CORREIA E, PAULO CM, ANGULO L & VIEIRA JAG. 2020. Ionospheric response to the June 2015 geomagnetic storm in the South American region. Adv Space Res 65: 2172-2183. doi: 10.1016/j.asr.2020.02.025.

MACOTELA EL, RAULIN J-P, MANNINEN J, CORREIA E, TURUNEN T & MAGALHÃES A. 2017. Lower ionosphere sensitivity to solar X-ray flares over a complete solar cycle evaluated

from VLF signal measurements. J Geophys Res-Space 122: 12,370-12,377. doi: 10.1002/2017JA024493.

MAKHMUTOV VS, RAULIN JP, DE MENDONÇA RRS, BAZILEVSKAYA GA, CORREIA E, KAUFMANN P, MARUN A, FERNANDEZ G & ECHER E. 2013. Analysis of cosmic ray variations observed by the CARPET in association with solar flares in 2011-2012. J of Phys Conf Ser (Online) 409: 1/012185-4. doi: 10.1088/1742-6596/409/1/012185.

MCRAE WM & THOMSON NR. 2004. Solar flare induced ionospheric D-region enhancements from VLF phase and amplitude observations. J Atmos Terr Phys 66: 77-87. https://doi.org/10.1016/j.jastp.2003.09.009.

MUELLA MTAH, DUARTE-SILVA MH, MORAES AO, DE PAULA ER, DE REZENDE LFC, ALFONSI L & AFFONSO BJ. 2017. Climatology and modeling of ionospheric scintillations and irregularity zonal drifts at the equatorial anomaly crest region. Ann Geophys 35: 1201-1218. doi: 10.5194/angeo-35-1201-2017.

NICOLET M & AIKIN AC. 1960. The Formation of the D-Region of the Ionosphere. J Geophys Res 65(5): 1469-1483. doi: 10.1029/JZ065i005p01469.

PACINI AA & RAULIN J-P. 2006. Solar X-ray flares and ionospheric sudden phase anomalies relationship: A solar cycle phase dependence. J Geophys Res 111: A09301. doi: 10.1029/2006JA011613.

PETER WB & INAN US. 2004. On the occurrence and spatial extent of electron precipitation induced by oblique nonducted whistler waves. J Geophys Res 109: A12215. doi: 10.1029/2004JA010412.

PILLAT VG, GUIMARAES LNF, FAGUNDES PR & DA SILVA JDS. 2013. A computational tool for ionosonde CADI's ionogram analysis. Computat Geosci 52(3): 372-378. doi: 10.1016/j.cageo.2012.11.009.

PRIKRYL P ET AL. 2016. GPS phase scintillation at high latitudes during the geomagnetic storm of 17-18 March 2015. J Geophys Res-Space 121: 10448-10465. doi:10.1002/2016JA023171.

RAULIN J-P, DAVID P, HADANO R, SARAIVA ACV, CORREIA E & KAUFMANN P. 2009. The South America VLF NETwork (SAVNET). Earth Moon Planets 104: 247-261. doi: 10.1007/s11038-008-9269-4.

RAULIN J-P, PACINI AA, KAUFMANN P, CORREIA E, APARECIDA G & MARTINEZ M. 2006. On the detectability of solar X-ray flares using very low frequency sudden phase anomalies. J Atmos Terr Phys 68: 1029-1035. doi: 10.1016/j.jastp.2005.11.004.

RAULIN J-P ET AL. 2010. Solar flare detection sensitivity using the South America VLF Network (SAVNET). J Geophys Res 115: A07301. doi:10.1029/2009JA015154.

RAULIN J-P, TROTTET G, GIMÉNEZ DE CASTRO CG, CORREIA E & MACOTELA EL. 2014. Nighttime sensitivity of ionospheric VLF measurements to X-ray bursts from a remote cosmic source. J Geophys Res-Space 119: 4758-4766. doi:10.1002/2013JA019670.

SCHERRER D, COHEN M, HOEKSEMA T, INAN U, MITCHELL R & SCHERRER P. 2008. Distributing space weather monitoring instruments and educational materials worldwide for IHY 2007: The AWESOME and SID project. Adv Space Res 42: 1777-1785. doi: 10.1016/j.asr.2007.12.013.

SPOGLI L, ALFONSI L, CILLIERS P, CORREIA E, DE FRANCESCHI G, MITCHELL CN, ROMANO V, KINRADE J & CABRERA MA. 2013. Ann Geophys 56: R0220-1-R0220-12. doi: 10.4401/ag-6240.

SPOGLI L, ALFONSI L, DE FRANCESCHI G, ROMANO V, AQUINO MHO & DODSON A. 2009. Ann Geophys 27: 3429-3437. doi: 10.5194/angeo-27-3429-2009.

THOMAS EG, BAKER JBH, RUOHONIEMI JM, CLAUSEN LBN, COSTER AJ, FOSTER JC & ERICKSON PJ. 2013. Direct observations of the role of convection electric field in the formation of a polar tongue of ionization from storm enhanced density. J Geophys Res-Space 118: 1180-1189. doi: 10.1002/jgra.50116.

TSURUTANI B ET AL. 2004. Global dayside ionospheric uplift and enhancement associated with interplanetary electric fields. J Geophys Res-Space 109: A08302. doi: 10.1029/2003JA010342.

TSURUTANI BT ET AL. 2008. Prompt penetration electric fields (PPEFs) and their ionospheric effects during the great magnetic storm of 30–31 October 2003. J Geophys Res-Space 113: A05311. doi: 10.1029/2007JA012879.

VAN DIERENDONCK AJ, KLOBUCHAR J & HUA Q. 1993. In: ION GPS-93 Proceedings of the Sixth International Technical Meeting of the Satellite Division of the Institute of navigation, 22–24 September 1993, Salt Lake City, USA, p. 1333-1342.

WAIT JR & SPIES K. 1964. Characteristics of the Earth-Ionosphere Waveguide For VLF Radio Waves. NBS Technical Note, 300. National Bureau of Standard, Gaithersburg, Md.

WOODS TN, TOBISKA WK, ROTTMAN GJ & WORDEN JR. 2000. Improved solar Lyman a irradiance modeling from 1947 through 1999 based on UARS observations. J Geophys Res 105: 27195-27215. doi: 10.1029/2000JA000051.

How to cite
CORREIA E, FERNANDEZ JH, BAGESTON JV, MACHO EP & RAUNHEITTE LTM. 2022. Highlights of ionospheric investigations at Comandante Ferraz Brazilian Antarctic Station. An Acad Bras Cienc 94: e20210600. DOI 10.1590/0001-3765202220210600.

Manuscript received on April 26, 2021;
accepted for publication on July 5, 2021

EMILIA CORREIA[1,2]
https://orcid.org/0000-0003-4778-3834

JOSÉ HENRIQUE FERNANDEZ[3]
https://orcid.org/0000-0001-7617-9711

JOSÉ VALENTIN BAGESTON[4]
https://orcid.org/0000-0003-2931-8488

EDUARDO P. MACHO[2]
https://orcid.org/0000-0002-0890-7008

LUÍS TIAGO M. RAUNHEITTE[2]
https://orcid.org/0000-0003-3684-7628

[1]Instituto Nacional de Pesquisas Espaciais (INPE), Divisão de Clima Espacial, Av. dos Astronautas, 1758, 12227-010 São José dos Campos, SP, Brazil

[2]Universidade Presbiteriana Mackenzie, Centro de Rádio Astronomia e Astrofísica Mackenzie, Rua da Consolação, 930, 01302-907 São Paulo, SP, Brazil

[3]Universidade Federal do Rio Grande do Norte (UFRN), Escola de Ciências e Tecnologia, Campus Universitário Lagoa Nova, 59078-970 Natal, RN, Brazil

[4]Instituto Nacional de Pesquisas Espaciais, Coordenação Espacial do Sul, Campus da Universidade Federal de Santa Maria, Av. Roraima, 1000, 97105-970 Santa Maria, RS, Brazil

Correspondence to: **Emilia Correia**
E-mail: ecorreia@craam.mackenzie.br

Author contributions

EC: conceptualization, supervision, original draft preparation, writing-reviewing and editing. JHF, JVB, EPM, LTMR: writing-reviewing the last version.